MJFAS
Malaysian Journal of Fundamental and Applied Sciences

Yaakob *et al.* | Malaysian Journal of Fundamental and Applied Sciences, Vol. 20 (2024) 779–789

RESEARCH ARTICLE

Theoretical Study on the Disparate Spatial Arrangement of 3',4',5,7-tetrahydroxy-3-flavene Towards Jack Bean Urease Enzyme Active Site

Mohd Hafiz Yaakob[a], Zaidi Ab Ghani[a], Shukor Sanim Mohd Fauzi[b], Norlin Shuhaime[a], Sharifah Zati Hanani Syed Zuber[c], Lee Sin Ang[a*]

[a]Faculty of Applied Sciences, Universiti Teknologi MARA Perlis Branch, Arau Campus, 02600 Arau, Perlis, Malaysia; [b]College of Computing, Informatics and Mathematics, Universiti Teknologi MARA Perlis Branch, Arau Campus, 02600 Arau, Perlis, Malaysia; [c]Faculty of Chemical Engineering Technology, Universiti Malaysia Perlis, Perlis, Malaysia

Abstract Urease enzyme plays crucial role in the hydrolysis of urea. Excessive hydrolysis of urea can have significant impacts on the environment. In recent years, there has been growing interest in identifying natural compounds that can inhibit urease activity. Flavonoids, phytochemical compounds present in plants, have shown promising potential as urease inhibitors. Studies have revealed that certain flavonoids, such as 3',4',5,7-tetrahydroxy-3-flavene, abbreviated as H4FLA for convenient, exhibit potent inhibition of urease, surpassing the efficacy of well-known synthetic inhibitors. In the present study, we report quantum mechanical calculations that mainly investigate the interaction of H4FLA towards urease at disparate spatial arrangement. It was found that the most favourable position between H4FLA and active site of urease has interaction energy of –3.80 eV. Topology analysis revealed that there is no typical covalent bond found between atoms involved in the interaction. Only weak interactions were detected. The hydroxyl groups with highest (negative) local potential throughout the structure, contribute mainly to the formation of non-covalent interaction with the nickel centers, indicating their potential involvement in the inhibitory activity of flavonoids against urease.

Keywords: Urease, flavonoids, inhibitor, semiempirical, GFN2-xTB, topology.

Introduction

Urease is an enzyme that catalyzes the hydrolysis of urea into ammonia and carbon dioxide. This enzymatic reaction is of great significance in various biological processes, including nitrogen metabolism and the pathogenesis of certain microorganisms [1-3]. The hydrolysis of urea by urease enzyme is a rapid reaction, with the rate of reaction depends on the concentration of urease enzyme and urea substrate. The mechanism of urea hydrolysis by urease involves the binding of urea to the active site of the enzyme, followed by the transfer of a hydroxide ion to the urea molecule, resulting in the formation of ammonia and a carbamate intermediate [4,5]. The carbamate intermediate is then hydrolyzed to release ammonia and regenerate the active site of the enzyme [5-7]. According to previous studies, the rate of the hydrolysis reaction in the presence of urease is more than 10^{14} times higher compared to the uncatalyzed reaction [8,9]. This remarkable increase in reaction rate highlights the exceptional proficiency of urease as a catalyst.

However, excessive hydrolysis of urea can have significant detrimental impacts on the environment and human health [10-13]. Ammonia emissions from agricultural activities, such as the use of urea-based fertilizers, contribute to air pollution and lead to the formation of particulate matter and smog [14-16]. These emissions not only have environmental consequences but also pose health risks, as ammonia can irritate the respiratory system and contribute to the formation of secondary pollutants [17,18].

***For correspondence:**

anglee631@uitm.edu.my

Received: 23 Jan. 2024
Accepted: 11 June 2024

Additionally, excessive hydrolysis of urea can result in the loss of nitrogen, an essential nutrient for plant growth [19-21]. This may lead to reduce agricultural productivity and the need for increased fertilizer application, further exacerbating environmental issues. Furthermore, the release of excess ammonia into water bodies can contribute to eutrophication, leading to algal blooms and oxygen depletion, which could harm aquatic ecosystems [22,23]. Therefore, it is crucial to manage and regulate the urease activity to minimize its environmental impact and ensure sustainable agricultural practices.

Flavonoids are a class of natural compounds known for their diverse biological activities, including their potential as urease inhibitors [24-26]. The study of the molecular interaction between the flavonoids inhibitors and urease enzyme active site has gained significant attention in recent years. Several studies have focused on investigating the binding interactions and inhibitory mechanisms of flavonoids such as hydrazine-carboxamide, isoflavones, and morin derivatives, with the urease enzyme [25-29]. The research explored the chemistry and mechanism of urease inhibition, highlighting the role of non-covalent interactions such as hydrogen bonds and hydrophobic contacts in stabilizing the enzyme-inhibitor complexes.

An important thing to bear mind when working with urease active site is that the urease active site consists of two divalent nickel ions that are separated by ca. 3.5 Å, with a hydroxide as bridging ligand (labelled as WB in literature) and few histidine, lysine, cysteine and aspartate residues [2,30-32]. The inhibition of urease occurs from the interaction of inhibitor around the nickel centers and residues, confirmed by numerous studies. For instance, researcher reported that urease inhibition can be achieved by formation of urease-benzoquinone covalent complex at the cysteine residue and the presence of ionic interactions between sulfhydryl groups with nitrogen and oxygen donor atoms of histidine [33,34]. Additionally, synthesized dithiobisacetamides as urease inhibitor, reported to bind with urease without covalent modification to the residue, indicating non-covalent binding to urease inhibition mechanism [35]. To study all these interactions in a large system by computational approach seems to be quite tough. However, the development of new computational methods has made possible to the study of large system such as urease enzyme complexes within a reasonable time. Here, GFN2-xTB semiempirical quantum mechanics simulations were applied, due to its computational efficiency, fast and can be reasonably accurate for transition metal complexes and protein structures [36-39].

In addition to its accuracy and versatility, the GFN2-xTB method offers significant cost-cutting benefits compared to traditional all-electron density functional theory (DFT) calculations. By employing a more efficient semi-empirical approach, GFN2-xTB reduces computational expenses without compromising the quality of results [40-42]. This cost-effectiveness is particularly advantageous for large-scale studies or high-throughput screening processes, where computational resources are often a limiting factor. Furthermore, the streamlined computational requirements of GFN2-xTB enable researchers to explore a broader range of chemical systems and phenomena within realistic timeframes and budget constraints. Thus, the adoption of GFN2-xTB presents a compelling opportunity to enhance research productivity and accelerate scientific discovery while optimizing resource allocation.

The present study focuses on the binding mode of H4FLA at disparate spatial arrangement to the nickel ions of urease enzyme active site, hence, we wish to provide valuable structural and electronic insights into the urease-inhibitor interaction. In this study, the size of the urease active site was increased by considering a few more residues to capture more realistic conditions of the active site. This modification aimed to enhance the enzyme's ability to accommodate and interact with substrates in a manner that better reflects the natural environment.

Models and Computational Methods

Jack bean urease (JBU) or scientifically addressed as *Canavalia Ensiformis* enzyme was selected due to its high ureolytic activity. It is reported that JBU exhibited ureolytic activity as high as 2700-3500 μmol urea/min mg depending on the purity and condition of the enzyme [4,43]. The 3LA4 JBU crystal structure from RCSB Protein Data Bank was selected to be used in this study due to the stated less than 10% difference between R-free and R-work value, as it is considered as a high-resolution structure and provides exact insights into the protein's structure and function [44-46]. For flavonoids inhibitor structure, 3',4',5,7-tetrahydroxy-3-flavene (denoted as H4FLA) was chosen due to its low half maximal inhibitory concentration (IC_{50}) value (IC_{50} = 4.42 ± 0.31 μM) [26]. The structure was retrieved from Cambridge Structural Database (CSD) [47]. The structure of JBU's active site and H4FLA are shown in Figure 1.

It was reported that the enzyme's catalytic activity takes place in the active site where dinickel metals are located [29,48,49]. Hence, the 3LA4 JBU crystal structure was truncated to form active site with the

following residues His407, His409, Lys490, His492, Asp494, His519, His545, Cys592, His593, Arg609, Asp633 and Ala636 retained [45,50,51]. The urease active site model after modification contained 239 atoms. Both structures of the urease active site and H4FLA were processed by PyRx 0.8, a virtual screening software for molecular docking [52]. Docking was performed to get the preferred orientation of H4FLA into the surrounding of urease's active site. Five docked spatial arrangements with lowest binding free energy were analyzed using the Avogadro molecular graphics system (version 1.2.0) and labelled as P1 to P5. The structures were verified using GaussView (version 5.0.9), to address any improper issues with the atoms and bonds before submitted to the quantum theoretical calculations.

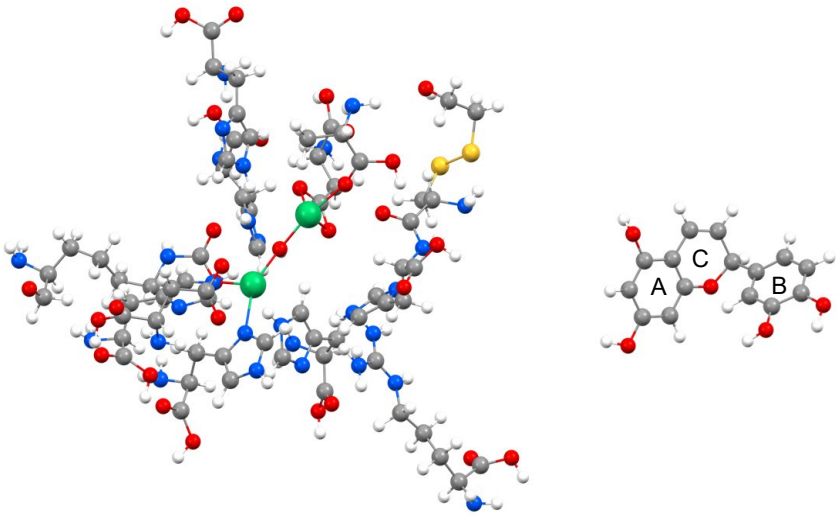

Figure 1. Chemical structures of JBU's active site (left) and H4FLA inhibitor (right). The nickel ions are represented in green, while CPK coloring is used for all other atoms. The phenyl rings (A and B) and a heterocyclic ring (C) of H4FLA are labelled for components identification. Due to the complexity and cluttered nature, overlapping images of P1 to P5 of H4FLA were not shown in this diagram

All geometry and energy calculations were performed using GFN2-xTB method, a semiempirical approach implemented in the xTB software version 6.6.1 [38]. All the computational setups are set to default values. All atoms in the system were freezed except two nickel ions, the bridging hydroxide ions between two nickel and the inhibitor molecule as they play crucial role in the catalytic mechanism of urease in the hydrolysis process.

To measure the interaction strength between urease and H4FLA at the specific arrangements, the interaction energy (E^{int}) between the JBU's active site and the H4FLA was calculated by Equation 1:

$$E^{int} = E_{urease+H4FLA} - E_{urease} - E_{H4FLA} \quad (1)$$

Electrostatic potential (ESP) and quantum theory of atoms in molecules (QTAIM) analysis of the optimized complexes were performed by Multiwfn, which is a multifunctional wavefunction analysis program developed by Tian Lu and Chen [53]. Both ESP and QTAIM are critical for predicting and characterizing chemical bond and the intermolecular interactions between the urease active site and H4FLA. The observations into specific bond critical points (BCPs) enables the qualitative analysis on the types of chemical bonding, i.e., covalent, ionic, van der Waals, hydrogen. Main topology parameters such as electron density ρ(r), potential energy density V(r), Laplacian of electron density $\nabla^2\rho$(r), energy density H(r) were all obtained through the Multiwfn software.

Results and Discussion

Geometrical Structure and Interaction Energy of Urease-Flavonoids

In this study, the performance of the GFN2-xTB method is compared to the DFT method of B3LYP/6-31G**. No imaginary frequencies were found from geometry optimization of both level of theory. The GFN2-xTB method yields slight changes to the value of interaction energy and these findings are in line with those found in literature, hence support that GFN2-xTB are suitable for optimizing molecular structures for various chemical applications. The interaction energies for all system and the interatomic distances of significant atoms for the interaction are shown in Table 1 and Table 2 respectively. The interaction between JBU active site and H4FLA are favourable at all positions due to the negative interaction energy. The more negative the interaction energy value, the more thermodynamically favourable the interaction.

The interaction energy for all the complexes ranges from –2.33 to –3.80 eV. The results show that it is comparable to the NBPT commercial urease inhibitor, which was found to have interaction energy of –1.68 eV [54]. The most favourable interaction is at P2 with interaction energy of –3.80 eV, while the least favourable interaction at P5 with interaction energy of –2.33 eV. This may be due to the higher number of interactions occurs between H4FLA and JBU active site in P2, as it was observed that the position of ring B approached towards the residues while in P5, the ring B was pointed out to the area with least residues of the complexes.

The optimized structures of H4FLA inhibitor at P2 and P5 position in the urease-flavonoids complexes are shown in Figure 2. The other positions (P1, P3 and P4) have configurations that are in between P2 and P5. Two hydroxyl (–OH) groups at ring A, as shown in Figure 3, has been observed to initiate the interaction with JBU active site due to its ability to chelate with Ni atoms. The spatial arrangement of H4FLA has been found to have a significant impact on their interaction and it is consistent to previous study which suggest that the –OH group strongly interacts with the enzyme, providing the main binding affinity for ligand-urease complex [25,26]. The interatomic distances between –OH groups of H4FLA and two Ni atoms also seems to shift the interaction energy generated from the complex. From the results, shorter interatomic distances around the Ni atoms causes an increase in the interaction energy. The atomic distance between Ni atoms and –OH group were much shorter for P2 compared to the other system such as Ni_1-O_5 (distance = 2.36 Å) and Ni_2-O_7 (distance = 3.81 Å) interaction after optimization, as shown in Table 2. This result suggests that the interplay between these atoms also contributed to the stability of the complex. This effect may have important implications for understanding and developing potent inhibitor in the future.

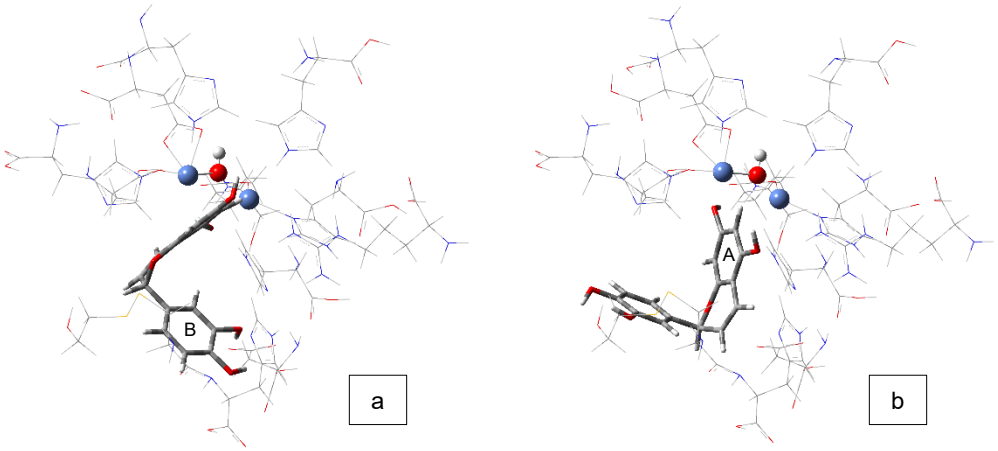

Figure 2. Optimized structures of urease-H4FLA complexes at P2 (a) and P5 (b) arrangement by the GFN2-xTB method; blue spheres: nickel ions, red and white spheres; hydroxide ion, wireframe: urease active site residues, tube: H4FLA

Table 1. Interaction energies (E^{int}, eV) for H4FLA with JBU active site at various positions (P1-P5) by GFN2-xTB and B3LYP/6-31G** method

Position	E^{int} (eV), GFN2-xTB	E^{int} (eV), B3LYP/6-31G**
P1	–2.36	–2.33
P2	–3.80	–2.88
P3	–2.48	–2.58
P4	–2.88	–2.68
P5	–2.23	–1.58

Table 2. Interatomic distances between hydroxyl groups in ring A of H4FLA with two nickel atoms and bridging hydroxide at the center of JBU active site

Position	Interatomic distances, *r* (Å)							
	Ni_1-O_5	Ni_1-O_7	Ni_2-O_5	Ni_2-O_7	O_1-O_5	O_1-O_7	H_1-O_5	H_1-O_7
P1	2.37(3.55)	5.78(3.89)	3.15(3.42)	3.48(4.81)	2.57(2.89)	2.57(2.89)	3.51(3.65)	5.20(3.57)
P2	2.36(2.40)	5.38(4.87)	3.01(2.67)	3.81(6.05)	2.57(2.03)	4.59(5.42)	3.49(2.28)	5.14(4.58)
P3	5.15(5.00)	3.73(2.59)	6.27(6.96)	2.12(2.21)	5.48(6.11)	4.59(3.25)	3.51(4.21)	5.07(2.76)
P4	2.35(4.53)	5.62(3.28)	3.12(3.47)	4.59(4.03)	2.57(3.43)	4.59(3.25)	3.51(4.21)	5.07(2.76)
P5	5.46(5.39)	3.24(2.72)	4.69(6.71)	2.23(2.16)	4.89(6.21)	2.58(1.94)	5.74(6.42)	3.28(2.63)

*The values in the brackets are before the optimization.

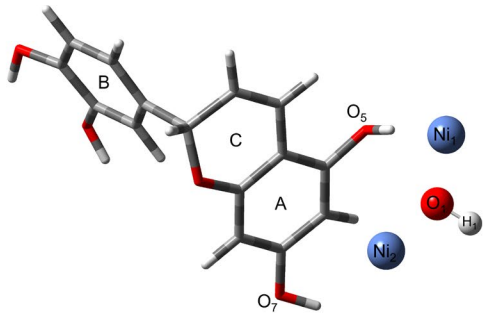

Figure 3. Close-up and labelled of the H4FLA structure with nickel and bridging hydroxide of the JBU active site (original image captured from Figure 2(a) and rearranged for better view)

ESP Analysis

Electrostatic potential (ESP) analysis is essential for understanding the electronic properties and reactivity of molecule. In this study, ESP analysis was applied to investigate the reactivity behaviour of H4FLA to the JBU active site. Based on the optimized structures, the ESP surface of H4FLA was obtained and is shown in Figure 4. The positive and negative electrostatic potentials are represented by the red and blue surfaces, respectively. The electrostatic potential increases with the intensity of the colour. From the figure, it was observed that the negative potential of H4FLA mostly located near the O atom of the hydroxyl group at ring A and ring C with three lowest ESP minima value scattered around the flavonoid's backbone. The significant ESP minima of O atom at ring A are –47.39, –44.07 and ring C, are –43.57, –42.87 kcal/mol, respectively. Each surface maximum in the H4FLA structure corresponds to hydrogen, which most of the points are distributed at ring B. The significant surface maximum of H atom on H4FLA are +55.41, +51.02, +50.23, and +47.52 kcal/mol.

For H4FLA structure, the reactivity towards the JBU active site, specifically on the ring (ring A, B and C)

to the nickel centres, are predicted from the ESP minima value of the O atoms. From ESP results, the negative surface regions at atoms O of ring A were slightly negative to the atoms O of ring C. The evaluation of this analysis appears to tally with the docking results where ring A was pointing into the nickel centres. High numbers of negative points at ring A and B, make them to be more repulsive to the positive nickel centres than ring C and, accountable to nucleophilic attacks in the inhibition mechanism.

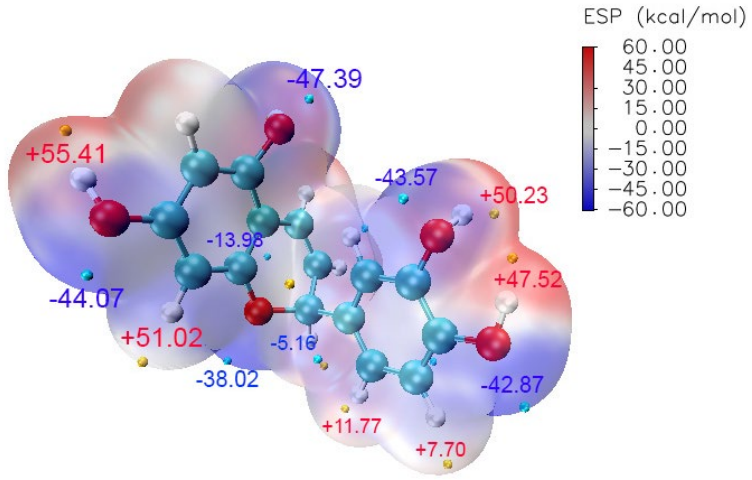

Figure 4. ESP-mapped molecular vdW surface of H4FLA inhibitor obtained at GFN2-xTB level (electron density isovalue = 0.001 a.u.). The unit is in kcal/mol. Surface local minima and maxima of ESP are represented as small cyan and orange spheres, respectively. The local surface maxima with negative ESP values are meaningless and thus not shown

QTAIM Analysis

QTAIM approach was applied on the electron density of the H4FLA-JBU relaxed complexes, as to analyze the interaction between H4FLA and JBU active site. In this regard, bond critical points (BCPs) that rationalizes bonding between the parts of the urease and H4FLA were found. All the probable critical points were identified as verified by the Poincarè-Hopf relationship. The analysis focus on explaining the effect of spatial arrangement of H4FLA into the JBU active site which creates specific interaction between the hydroxyl group and Ni atoms towards the surrounding residues. The values of selected topological properties for interaction at P2 (the strongest E^{int}) and P5 (the weakest E^{int}) position are gathered in Table 3.

Based on available data, it can be confirmed that there is no formation of new typical covalent bond from the interaction between H4FLA and JBU active site at all positions, based on the classification of interatomic interactions analysis proposed by Espinosa *et al*. [55]. This observation agrees with findings in Awllia *et al*. [24] and Kataria et al. [27] indicating the absence of covalent bonds in the inactivation of urease by flavonoids. As seen in Figure 5, there is no BCPs detected in pure shared shell region (region III) that contribute to typical covalent bond formation, merely all critical points were distributed across the pure closed shell (region I) and transit closed shell (region II) which indicates the presence of ionic bonds, hydrogen bonds and van der Waals interaction. This pattern has been observed previously with B3LYP functional with the double-ζ 6-31G* basis set and molecular docking studies [56-60].

Possible reasons for what may cause the difference of interaction energy between different arrangements of the complexes were further investigated through the behaviour of specific BCPs in Figure 5. From the H4FLA-Ni interaction, in region III, it is found that P5 BCPs (orange triangle) exhibit weaker CD magnitude than P2, indicate that there is weaker interaction between H4FLA and JBU active site. For the H4FLA-residues interaction, P5 BCPs (orange triangle) exhibit greater SD magnitude which represent weaker interaction. Due to this, P5 has lower interaction energy. From the QTAIM analysis, the study now provides evidence to implications between the position of H4FLA towards the interaction with JBU active site.

Table 3. Selected topological parameters for interaction between H4FLA and urease active site at P2 and P5 position, calculated using GFN2-xTB on the optimized geometry

Interatomic BCPs	ρ_b (e/A^3)[a]	$\nabla^2\rho_b$ (e/A^5)[b]	G_b/ρ_b (h e^{-1})[c]	H_b/ρ_b (h e^{-1})[d]	$\lvert V_b\rvert/G_b$[e]
H4FLA-P2					
Ni33-O28	0.302	7.097	1.503	256.534	0.935
Ni96-C27	0.332	5.259	1.114	-145.040	1.050
Ni33-N218	0.415	8.449	1.420	-170.181	1.046
Ni96-O160	0.462	11.793	1.804	-473.481	1.100
Ni33-O56	0.595	11.281	1.423	-515.110	1.138
Ni96-O56	0.805	11.974	1.288	-1169.691	1.346
Ni33-O166	0.717	14.245	1.587	-902.530	1.217
Ni96-O148	0.617	12.377	1.533	-644.811	1.160
Ni96-O149	0.392	9.037	1.554	6.611	0.998
O6-C59	0.026	0.763	1.423	1717.247	0.540
N231-O29	0.013	0.368	1.289	1671.774	0.506
H4FLA-P5					
N207-Ni130	0.566	10.861	1.443	-483.757	1.128
Ni130-O60	0.646	12.457	1.475	-571.013	1.147
Ni130-O62	0.705	13.949	1.573	-871.032	1.211
O8-Ni98	0.385	8.810	1.537	-18.479	1.005
O176-Ni98	0.318	8.364	1.729	-43.940	1.010
Ni98-O60	0.926	13.619	1.334	-1494.117	1.426
Ni98-O164	0.490	11.682	1.684	-204.146	1.046
Ni98-O165	0.631	11.950	1.468	-739.310	1.192
O8-O65	0.066	1.309	1.063	849.667	0.695
O268-O28	0.014	0.345	1.155	1502.540	0.505
O232-O14	0.009	0.344	1.760	2253.913	0.512

[a]Electron density at the BCP, [b]Laplacian of the electron density at the BCP, [c]Lagrangian kinetic energy density ratio at the BCP, [d]Total energy density ratio at the BCP, [e]V_b is the potential energy density

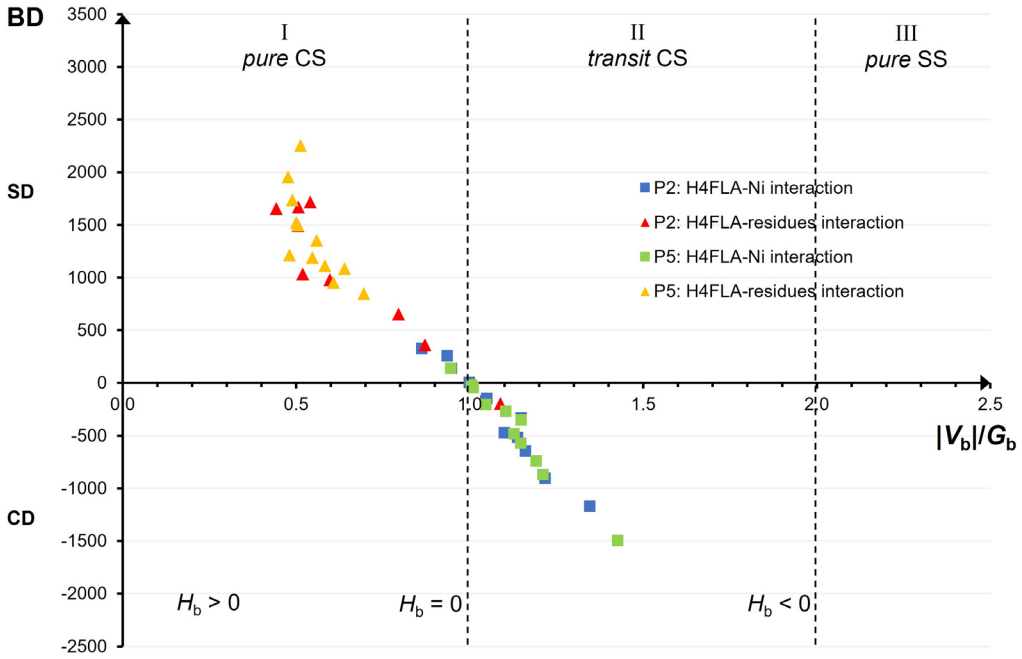

Figure 5. Theoretical bond degree parameter (BD = H_b/ρ_b) as a function of $|V_b|/G_b$ plot of P2 and P5 positions optimized by GFN2-xTB. The square and triangle represent, respectively, H4FLA-Ni and H4FLA-residues interactions

Conclusions

This work provides overview of the interaction of flavonoids inhibitor, 3',4',5,7-tetrahydroxy-3-flavene (H4FLA) with urease enzyme by semiempirical GFN2-xTB tight binding method. The findings underscore the important contribution of theoretical approaches in identifying the favourable position of the flavonoids into the urease active site complex structure, thereby aiding in the development of potential inhibitor. Among the different spatial arrangement of H4FLA towards the enzyme, it was found that the most favourable interaction is at P2 with interaction energy of –3.80 eV. Topology analysis revealed that there are several non-covalent interactions, including hydrogen bonds and van der Waals forces that stabilize the enzyme-inhibitor complex, but does not engage in covalent interaction with the nickel atoms. Hence, flavonoids use in this study can act as urease inhibitor which has been proven experimentally, and now computationally supported. Our findings underscore the importance of utilizing GFN2-xTB for geometry optimization, thereby enabling subsequent investigations into electronic properties using more computationally intensive methods such as DFT. By providing a clear guideline for researchers, this work paves the way for enhanced understanding and exploration of complex molecular systems.

Conflicts of Interest

The author(s) declare(s) that there are no conflicts of interest regarding the publication of this paper.

Acknowledgement

The authors would like to acknowledge Universiti Teknologi MARA for the support during the study.

References

[1] Karplus, P. A., Pearson, M. A., & Hausinger, R. P. (1997). 70 years of crystalline urease: What have we learned? *Accounts of Chemical Research, 30*(7), 330–337.

[2] Jabri, E., Carr, M. B., Hausinger, R. P., & Karplus, P. A. (1995). The crystal structure of urease from *Klebsiella aerogenes*. *Science, 268*(5210), 998–1004.

[3] Kappaun, K., Piovesan, A. R., Carlini, C. R., & Ligabue-Braun, R. (2018). Ureases: Historical aspects, catalytic, and non-catalytic properties – A review. *Journal of Advanced Research, 13*, 3–17.

[4] Krajewska, B. (2009). Ureases I. Functional, catalytic, and kinetic properties: A review. *Journal of Molecular Catalysis B: Enzymatic, 59*(1-4), 9–21.

[5] Estiu, G., & Merz, K. M. (2004). The hydrolysis of urea and the proficiency of urease. *Journal of the American Chemical Society, 126*(22), 6932–6944.

[6] Amtul, Z., Atta ur, R., Siddiqui, R. A., & Choudhary, M. I. (2002). Chemistry and mechanism of urease inhibition. *Current Medicinal Chemistry, 9*(12), 1323–1348.

[7] Domínguez, M. J., Sanmartín, C., Font, M., Palop, J. A., San Francisco, S., Urrutia, O., Houdusse, F., & García-Mina, J. M. (2008). Design, synthesis, and biological evaluation of phosphoramide derivatives as urease inhibitors. *Journal of Agricultural and Food Chemistry, 56*(11), 3721–3731.

[8] Daneshfar, A., Matsuura, T., Emadzadeh, D., Pahlevani, Z., & Ismail, A. F. (2015). Urease-carrying electrospun polyacrylonitrile mat for urea hydrolysis. *Reactive and Functional Polymers, 87*, 37–45.

[9] Russell, A. J., Erbeldinger, M., DeFrank, J. J., Kaar, J., & Drevon, G. (2002). Catalytic buffers enable positive-response inhibition-based sensing of nerve agents. *Biotechnology and Bioengineering, 77*(4), 352–357.

[10] Chu, Q., Xue, L., Cheng, Y., Liu, Y., Feng, Y., Yu, S., Meng, L., Pan, G., Hou, P., Duan, J., & Yang, L. (2020). Microalgae-derived hydrochar application on rice paddy soil: Higher rice yield but increased gaseous nitrogen loss. *Science of The Total Environment, 717*, 137127.

[11] Chen, A., Lei, B., Hu, W., Lu, Y., Mao, Y., Duan, Z., & Shi, Z. (2015). Characteristics of ammonia volatilization on rice grown under different nitrogen application rates and its quantitative predictions in Erhai Lake Watershed, China. *Nutrient Cycling in Agroecosystems, 101*(1), 139–152.

[12] Qi, S., Ding, J., Yang, S., Jiang, Z., & Xu, Y. (2022). Impact of biochar application on ammonia volatilization from paddy fields under controlled irrigation. *Sustainability, 14*(3), 1337.

[13] Zhang, P., Wu, T., Cao, H., Zhang, J., James, T. D., & Sun, X. (2023). Fluorometric detection of volatile amines using an indanonalkene platform. *Organic Chemistry Frontiers, 10*(8), 1393–1398.

[14] Gu, B., Sutton, M. A., Chang, S. X., Ge, Y., & Chang, J. (2014). Agricultural ammonia emissions contribute to China's urban air pollution. *Frontiers in Ecology and the Environment, 12*(5), 265–266.

[15] Piwowar, A. (2020). Farming practices for reducing ammonia emissions in Polish agriculture. *Atmosphere, 11*(12), 1353.

[16] Pleim, J. E., Ran, L., Appel, W., Shephard, M. W., & Cady-Pereira, K. (2019). New bidirectional ammonia flux model in an air quality model coupled with an agricultural model. *Journal of Advances in Modeling Earth Systems, 11*(10), 2934–2957.

[17] Sun, C., Hong, S., Cai, G., Zhang, Y., Kan, H., Zhao, Z., Deng, F., Zhao, B., Zeng, X., Sun, Y., Qian, H., Liu, W., Mo, J., Guo, J., Zheng, X., Su, C., Zou, Z., Li, H., & Huang, C. (2021). Indoor exposure levels of ammonia in residences, schools, and offices in China from 1980 to 2019: A systematic review. *Indoor Air, 31*(6), 1691–1706.

[18] Phillips, C. J. C., Pines, M. K., Latter, M., Muller, T., Petherick, J. C., Norman, S. T., & Gaughan, J. B. (2010). The physiological and behavioral responses of steers to gaseous ammonia in simulated long-distance transport by ship. *Journal of Animal Science, 88*(11), 3579–3589.

[19] Cantarella, H., Otto, R., Soares, J. R., & Silva, A. G. D. (2018). Agronomic efficiency of NBPT as a urease inhibitor: A review. *Journal of Advanced Research, 13*, 19–27.

[20] San Francisco, S., Urrutia, O., Martin, V., Peristeropoulos, A., & Garcia-Mina, J. M. (2011). Efficiency of urease and nitrification inhibitors in reducing ammonia volatilization from diverse nitrogen fertilizers applied to different soil types and wheat straw mulching. *Journal of the Science of Food and Agriculture, 91*(8), 1569–1575.

[21] Patra, A. K., & Aschenbach, J. R. (2018). Ureases in the gastrointestinal tracts of ruminant and monogastric animals and their implication in urea-N/ammonia metabolism: A review. *Journal of Advanced Research, 13*, 39–50.

[22] Smith, V. H., Tilman, G. D., & Nekola, J. C. (1999). Eutrophication: Impacts of excess nutrient inputs on freshwater, marine, and terrestrial ecosystems. *Environmental Pollution, 100*(1-3), 179–196.

[23] Gao, J., Li, L., Hu, Z., Yue, H., Zhang, R., & Xiong, Z. (2016). Effect of ammonia stress on nitrogen metabolism of *Ceratophyllum demersum*. *Environmental Toxicology and Chemistry, 35*(1), 205–211.

[24] Awllia, J. A. J., Al-Ghamdi, M., Huwait, E., Javaid, S., Atia tul, W., Rasheed, S., & Choudhary, M. I. (2016). Flavonoids as natural inhibitors of Jack bean urease enzyme. *Letters in Drug Design & Discovery, 13*(3), 243–249.

[25] Liu, H., Wang, Y., Lv, M., Luo, Y., Liu, B. M., Huang, Y., Wang, M., & Wang, J. (2020). Flavonoid analogues as urease inhibitors: Synthesis, biological evaluation, molecular docking studies, and in-silico ADME evaluation. *Bioorganic Chemistry, 105*, 1–9.

[26] Xiao, Z. P., Peng, Z. Y., Dong, J. J., He, J., Ouyang, H., Feng, Y. T., Lu, C. L., Lin, W. Q., Wang, J. X., & Xiang, Y. P. (2013). Synthesis, structure–activity relationship analysis, and kinetics study of reductive derivatives of flavonoids as *Helicobacter pylori* urease inhibitors. *European Journal of Medicinal Chemistry, 63*, 685–695.

[27] Kataria, R., & Khatkar, A. (2019). Molecular docking, synthesis, kinetics study, structure–activity relationship, and ADMET analysis of morin analogues as *Helicobacter pylori* urease inhibitors. *BMC Chemistry, 13*, 45.

[28] Saito, T., & Takano, Y. (2022). QM/MM molecular dynamics simulations revealed catalytic mechanism of urease. *The Journal of Physical Chemistry B, 126*(10), 2087–2097.

[29] Mazzei, L., Musiani, F., & Ciurli, S. (2020). The structure-based reaction mechanism of urease, a nickel-dependent enzyme: Tale of a long debate. *Journal of Biological Inorganic Chemistry, 25*(5), 829–845.

[30] Lee, J. K., Park, H. J., Cha, S. J., Kwon, S. J., & Park, J. H. (2021). Effect of pyroligneous acid on soil urease, amidase, and nitrogen use efficiency by Chinese cabbage (*Brassica campestris* var. *Pekinensis*). *Environmental Pollution, 291*, 118132.

[31] Estiu, G., & Merz, K. M. (2006). Catalyzed decomposition of urea: Molecular dynamics simulations of the binding of urea to urease. *Biochemistry, 45*(14), 4429–4443.

[32] Carter, E. L., Flugga, N., Boer, J. L., Mulrooney, S. B., & Hausinger, R. P. (2009). Interplay of metal ions and urease. *Metallomics, 1*(4), 207–214.

[33] Mazzei, L., Cianci, M., Musiani, F., & Ciurli, S. (2016). Inactivation of urease by 1,4-benzoquinone: Chemistry at the protein surface. *Dalton Transactions, 45*(16), 5455–5459.

[34] Hanif, M., Nawaz, M. A. H., Babak, M. V., Iqbal, J., Roller, A., Keppler, B. K., & Hartinger, C. G. (2014). Ruthenium(II)(η^6-arene) complexes of thiourea derivatives: Synthesis, characterization, and urease inhibition. *Molecules, 19*(6), 8080–8092.

[35] Liu, M.-L., Li, W.-Y., Fang, H.-L., Ye, Y.-X., Li, S.-Y., Song, W.-Q., Xiao, Z.-P., Ouyang, H., & Zhu, H.-L. (2022). Synthesis and biological evaluation of dithiobisacetamides as novel urease inhibitors. *ChemMedChem, 17*(11), e202100618.

[36] Rasmussen, M. H., & Jensen, J. H. (2020). Fast and automatic estimation of transition state structures using tight binding quantum chemical calculations. *PeerJ Physical Chemistry, 2*, e15.

[37] Bannwarth, C., Caldeweyher, E., Ehlert, S., Hansen, A., Pracht, P., Seibert, J., Spicher, S., & Grimme, S. (2021). Extended tight-binding quantum chemistry methods. *WIREs Computational Molecular Science, 11*(5), e1493.

[38] Bannwarth, C., Ehlert, S., & Grimme, S. (2019). GFN2-xTB—An accurate and broadly parametrized self-consistent tight-binding quantum chemical method with multipole electrostatics and density-dependent dispersion contributions. *Journal of Chemical Theory and Computation, 15*(3), 1652–1671.

[39] Schmitz, S., Seibert, J., Ostermeir, K., Hansen, A., Göller, A. H., & Grimme, S. (2020). Quantum chemical calculation of molecular and periodic peptide and protein structures. *The Journal of Physical Chemistry B, 124*(15), 3636–3646.

[40] Menzel, J. P., Kloppenburg, M., Belić, J., de Groot, H. J. M., Visscher, L., & Buda, F. (2021). Efficient workflow for the investigation of the catalytic cycle of water oxidation catalysts: Combining GFN-xTB and density functional theory. *Journal of Computational Chemistry, 42*(21), 1885–1894.

[41] Nurhuda, M., Perry, C. C., & Addicoat, M. A. (2022). Performance of GFN1-xTB for periodic optimization of metal-organic frameworks. *Physical Chemistry Chemical Physics, 24*(19), 10906–10914.

[42] Neugebauer, H., Bohle, F., Bursch, M., Hansen, A., & Grimme, S. (2020). Benchmark study of electrochemical redox potentials calculated with semiempirical and DFT methods. *The Journal of Physical Chemistry A, 124*(39), 7166–7176.

[43] Follmer, C., Barcellos, G. B. S., Zingali, R. B., Machado, O. L. T., Alves, E. W., Barja-Fidalgo, C., Guimarães, J. A., & Carlini, C. R. (2001). Canatoxin, a toxic protein from jack beans (*Canavalia ensiformis*), is a variant form of urease (EC 3.5.1.5): Biological effects of urease independent of its ureolytic activity. *Biochemical Journal, 360*(1), 217–224.

[44] Kleywegt, G. J., & Alwyn Jones, T. (1997). Model building and refinement practice. In *Methods in Enzymology* (pp. 208–230). Academic Press.

[45] Balasubramanian, A., & Ponnuraj, K. (2010). Crystal structure of the first plant urease from jack bean: 83 years of journey from its first crystal to molecular structure. *Journal of Molecular Biology, 400*(2), 274–283.

[46] Berman, H. M., Westbrook, J., Feng, Z., Gilliland, G., Bhat, T. N., Weissig, H., Shindyalov, I. N., & Bourne, P. E. (2000). The Protein Data Bank. *Nucleic Acids Research, 28*(1), 235–242.

[47] Groom, C. R., Bruno, I. J., Lightfoot, M. P., & Ward, S. C. (2016). The Cambridge Structural Database. *Acta Crystallographica Section B, 72*(2), 171–179.

[48] Mazinani, M., Behbehani, G. R., Gheibi, N., & Farasat, A. (2020). Study of jack bean urease interaction with luteolin by the extended solvation model and docking simulation. *AIMS Biophysics, 7*(4), 429–435.

[49] Klimczyk, M., Siczek, A., & Schimmelpfennig, L. (2021). Improving the efficiency of urea-based fertilization leading to reduction in ammonia emission. *Science of the Total Environment, 771*, 1–13.

[50] Carlsson, H., & Nordlander, E. (2010). Computational modeling of the mechanism of urease. *Bioinorganic Chemistry and Applications, 2010*, 1–8.

[51] Mazzei, L., Cianci, M., Contaldo, U., Musiani, F., & Ciurli, S. (2017). Urease inhibition in the presence of N-(n-butyl)thiophosphoric triamide, a suicide substrate: Structure and kinetics. *Biochemistry, 56*(27), 5391–5404.

[52] Dallakyan, S., & Olson, A. J. (2015). Small-molecule library screening by docking with PyRx. In *Methods in Molecular Biology* (Vol. 1263, pp. 243–250). Clifton, N.J.: Humana Press.

[53] Lu, T., & Chen, F. (2012). Multiwfn: A multifunctional wavefunction analyzer. *Journal of Computational Chemistry, 33*(5), 580–592.

[54] Azman, M. H. D., Sin, A. L., Zuber, S. Z. H. S., Yaakob, M. H., & Ghani, Z. A. (2021). Structural and electronic properties of NBPT inhibitor attached to urease. *Journal of Physics: Conference Series, 1874*, 012026.

[55] Espinosa, E., Alkorta, I., Elguero, J., & Molins, E. (2002). From weak to strong interactions: A comprehensive analysis of the topological and energetic properties of the electron density distribution involving X–H···F–Y systems. *The Journal of Chemical Physics, 117*(12), 5529–5542.

[56] Wan, L.-H., Jiang, X.-L., Liu, Y.-M., Hu, J.-J., Liang, J., & Liao, X. (2016). Screening of lipase inhibitors from *Scutellaria baicalensis* extract using lipase immobilized on magnetic nanoparticles and study on the inhibitory mechanism. *Analytical and Bioanalytical Chemistry, 408*(8), 2275–2283.

[57] Mohamed Yusof, N. I. S., Abdullah, Z. L., Othman, N., & Mohd Fauzi, F. (2022). Structure–activity relationship analysis of flavonoids and their inhibitory activity against BACE1 enzyme toward a better therapy for Alzheimer's disease. *Frontiers in Chemistry, 10,* 874615.

[58] Chaudhry, F., Naureen, S., Aslam, M., Al-Rashida, M., Rahman, J., Huma, R., Fatima, J., Khan, M., Munawar, M. A., & Ain Khan, M. (2020). Identification of imidazolylpyrazole ligands as potent urease inhibitors: Synthesis, antiurease activity, and in silico docking studies. *ChemistrySelect, 5*(46), 11817–11821.

[59] Mahmood, S.-U., Nazir, Y., Saeed, A., Abbas, Q., & Ashraf, Z. (2020). Synthesis, biological evaluation, and molecular docking studies of novel coumarinylthiazolyl imino-thiazolidinone hybrids as potent urease inhibitors. *ChemistrySelect, 5*(19), 5387–5390.

[60] Suárez, D., Díaz, N., & Merz, K. M. (2003). Ureases: Quantum chemical calculations on cluster models. *Journal of the American Chemical Society, 125*(49), 15324–15337.